Conf-9409178--5

LA-UR-94-3135

Title: **THE SYNCHRONOUS ACTIVE NEUTRON DETECTION SYSTEM FOR SPENT FUEL ASSAY**

Author(s): **M. M. Pickrell and P. K. Kendall**

Submitted to: **I&EC Special Symposium**
American Chemical Society
Atlanta, Georgia
September 19-21, 1994
(FULL PAPER)

Los Alamos
NATIONAL LABORATORY

Form No. 836 R5
ST 2629 10/91

DISCLAIMER

Portions of this document may be illegible in electronic image products. Images are produced from the best available original document.

THE SYNCHRONOUS ACTIVE NEUTRON DETECTION SYSTEM FOR SPENT FUEL ASSAY*

Mark M. Pickrell and Peter K. Kendall
Los Alamos National Laboratory
Los Alamos, NM 87545

ABSTRACT

We have begun to develop a novel technique for active neutron assay of fissile material in spent nuclear fuel. This approach will exploit the unique operating features of a 14-MeV neutron generator developed by Schlumberger.[1] This generator and a novel detection system will be applied to the direct measurement of the fissile material content in spent fuel in place of the indirect measures used at present.

The technique we are investigating is termed synchronous active neutron detection (SAND). It closely follows a method that has been used routinely in other branches of physics to detect very small signals in the presence of large backgrounds. Synchronous detection instruments are widely available commercially and are termed "lock-in" amplifiers.[2-4] We have implemented a digital lock-in amplifier in conjunction with the Schlumberger neutron generator to explore the possibility of synchronous detection with active neutrons. This approach is possible because the Schlumberger system can operate at up to a 50% duty factor, in effect, a square wave of neutron yield.

The results to date are preliminary but quite promising. The system is capable of resolving the fissile material contained in a small fraction of the fuel rods in a cold fuel assembly. It also appears to be quite resilient to background neutron interference. The interrogating neutrons appear to be nonthermal and penetrating. Although a significant amount of work remains to fully explore the relevant physics and optimize the instrument design, the underlying concept appears sound.

INTRODUCTION

The Spent Fuel Problem

Potential diversion of the fissile material in spent fuel is a significant problem in global nuclear materials management because of the sheer magnitude of the materials involved. For example, in the US, the first geologic repository for spent fuel is planned to contain 60 000 Mt of uranium and 500 Mt of plutonium from both defense and commercial fuel cycles. The problem is also international; presently 28 nations have commercial or defense nuclear power programs. Some, such as France, the UK, the FSU, and India, are actively pursuing reprocessing of spent fuel to extend the plutonium fuel cycle. This problem is complicated because as the spent fuel cools, it becomes less radioactive, less hazardous to handle, and a more attractive diversion target. In addition, repackaging of the spent fuel into containers lowers the probability of diversion detection using physical observation.[5-11]

The present technical approach for the nondestructive assay of spent fuel is an indirect measurement. A direct measurement is not performed because the radiation from the fissile material is overwhelmed by the radiation from fission products produced during exposure in the reactor core. Existing spent fuel assay systems, such as the passive Fork detector, measure the passive neutron and gamma emission from fission products such as ^{134}Cs, ^{137}Cs, ^{154}Eu, and ^{144}Ce-Pr. The fission product concentration is used to infer the exposure or burnup of the spent fuel. The burnup estimate is used with the declared initial enrichment to calculate the fissile plutonium and uranium content. The procedure is indirect and sensitive to several error sources such as the fuel irradiation history declared by the operator, the cooling off period since the fuel was removed, and the initial enrichment.[5-8, 10, 12-15]

Active neutron assay could alleviate these problems because it provides a direct measure of the fissile material. However, active neutron assay has been difficult because of the high ambient neutron emission from typical spent fuel. Two approaches have been tried with some success, but both are sensitive to the high-background-neutron rates. One approach is the ^{252}Cf shuffler. The basis for the shuffler is to irradiate a sample with an interrogating californium source, remove the source, and count the delayed fission neutrons. However, to adequately detect the induced, delayed neutrons above the background rate typical for spent fuel requires a large source, on the order of 10^9–10^{10} n/s. Even with large sources, this technique cannot measure highly radiating spent fuel.[16-19]

Another approach is the Fork detector combined with neutron multiplicity counting and an americium lithium photoneutron source. The americium lithium source interrogates the fuel sample with neutrons that have no multiplicity component because the neutron production process does not involve fission. The interrogating neutrons induce fissions in the sample, and these neutrons do have a multiplicity component. The real coincidence and multiplicity triples rate is measured by the multiplicity electronics and evaluated to determine the fissile material content. This method is also

*This work is supported by the US Department of Energy, Office of Nonproliferation and National Security, Office of Safeguards and Security.

limited to samples with low ambient neutron emission rates.[6,20,21]

The present IAEA criterion for spent fuel assay is to detect whether 10% of the rods are missing with at least a 90% confidence level. We wish to develop an active neutron-based assay system that measures fissile material directly, that can accommodate the entire range of ambient neutron interference possible from spent fuel, and that can satisfy the IAEA fiducial.

Issues for Active Neutron-Based Assay

The technical challenge of active neutron assay is to separate the induced fission neutrons from the interrogating neutrons and the ambient background. Historically, several approaches have been tried, such as the differential die-away (DDA) method, the californium shuffler, the active well coincidence counter (AWCC), and the related active Fork detector. The separation of the ambient background neutron rate from the fission neutron rate is done in a similar fashion for all these methods: by background subtraction. The method of separating the induced fission neutrons from the interrogating neutrons depends on the assay method, but is generally based on time separation. The Fork and AWCC detectors separate by time correlation, the shuffler separates by removing the source and counting delayed neutrons, and the DDA separates in time by waiting for the initial interrogating neutron burst to decay away in the detectors before counting.[6,8,10,13,18-26]

Another issue for active neutron assay is the average energy or temperature of the interrogating neutron spectrum. For the spent fuel application in particular, it is important to interrogate with nonthermal, energetic neutrons. The reason is that "cold" thermal neutrons have large fission cross sections, will not penetrate the fuel assembly, and will only sample a small portion of the fissile material.[27]

The SAND system, which we are developing, separates the induced neutrons from the ambient background in frequency and phase, rather than in time. The apparent benefits are a system that is more highly resistant to background interference, uses more penetrating "hot" neutrons for interrogation, and does not saturate the neutron detectors. This method is called synchronous detection and has been used routinely in many physics applications. In the SAND system, the neutron generator produces a square wave of neutrons, rather than a short pulse. Neutrons from induced fissions in the sample are counted using a multichannel time scaler, which counts individual neutrons in a stream of short time bins. The data from these time bins are used to implement a lock-in amplifier digitally. The frequency and phase component corresponding to the induced prompt fission neutrons is selected, and the other components are attenuated.

The Motivation for Synchronous Detection

The specific application for synchronous detection with active neutrons is to perform active neutron assay in a high-background environment. High-background count rates reduce the precision of active neutron assay, or in extreme cases render it impossible. The synchronous detection concept is one method for extracting a small, active signal in the presence of a large background. It has been routinely applied for the last several decades, although not with active neutrons.

The reason for trying this approach is the limitations with conventional background subtraction methods. Typically, background interference is reduced by narrowing the time window for counting signal neutrons. However, as the counting window is made more narrow to reduce the background interference, less signal is measured as well. The essential dichotomy is that a too narrow window eliminates both signal and noise, while a too large window encompasses more of the signal and also too much noise. For any particular case an optimum window can be chosen that balances these effects.

For neutron counting the fundamental limitation in a high-background environment is the minimum practical counting window. Ideally, if the assay signal could be made very narrow in time, then the counting window could be made narrow and the noise interference could be attenuated. The difficulty with this approach, however, is illustrated in Fig. 1. The neutron generator was programmed to produce a stream of narrow neutron pulses, and the time response (count rate) of the neutron detector was measured. Although the system was interrogated with a narrow pulse of neutrons, the response was a much broader decaying exponential. This behavior is characteristic of the detector die-away time. The conclusion is that even a short interrogating pulse cannot produce a short neutron signal. The counting time window must be nominally as large as the die-away time, and significant noise is also counted.

The benefit of using synchronous detections accrues by analyzing this system in the frequency domain, rather than the time domain. In discrete time, because of the symmetry properties of the discrete-time Fourier transform relations, there are an equal number of frequency bins and time bins. Just as a narrow neutron pulse might occupy a single time bin, a simple sine wave occupies a single frequency bin.

The significant aspect of the neutron detector is that it converts a narrow pulse of neutrons into a broad, decaying exponential in time, but a single frequency remains a single frequency. In the time domain many bins must be summed to capture the data. In the frequency domain a single frequency bin can be used. Therefore, if this system were interrogated with a sine wave of neutron yield, it would respond with a sine wave of neutron output. Both would occupy a single frequency bin. Of course, a sine wave of neutron yield

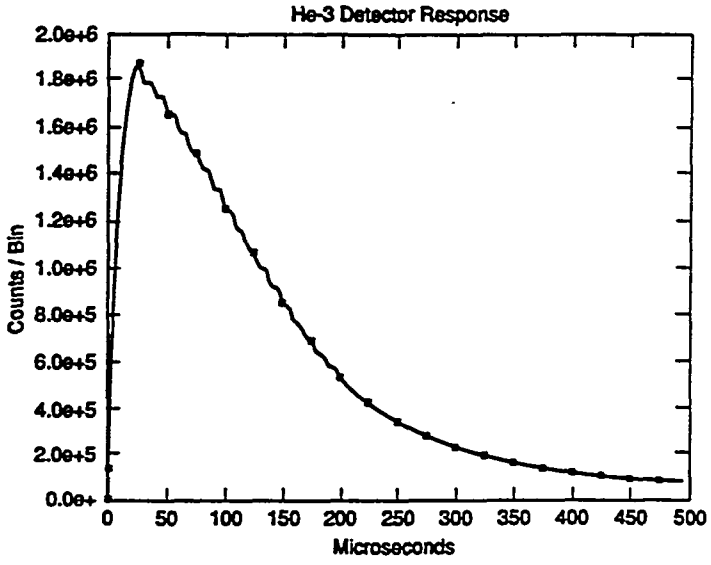

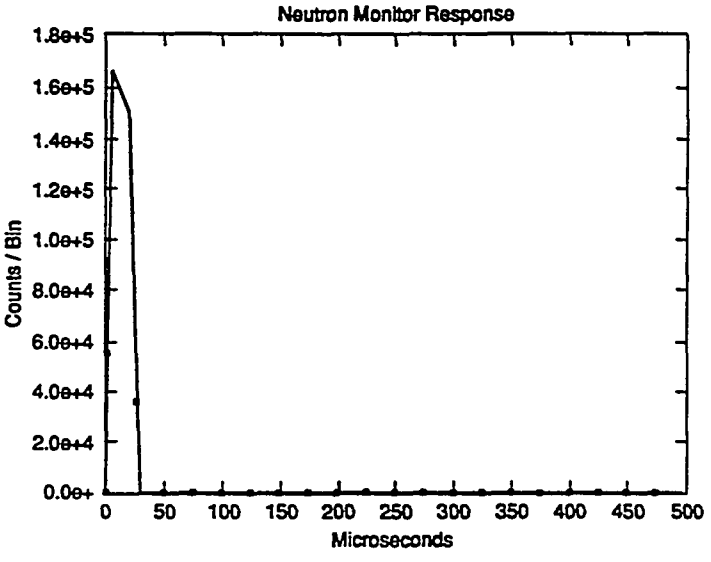

Fig. 1. Plots of a short neutron generator pulse and the detection system response, both as a function of time. For both plots, the accumulated counts in each of 100 time bins are plotted. Each time bin was 5 μs wide.

is impossible, but the Schlumberger neutron generator can produce a positive-definite square wave of output, and that is close enough. A single frequency bin is sufficient to capture the signal.

The background noise can also be evaluated in either the frequency or time domain. In the frequency domain, random (Poisson) noise is distributed evenly among the frequency bins (with a peak at the zero frequency component equal to the mean). Therefore, by using synchronous detection only a single bin is used to capture the signal and only a single bin of noise interferes with the measurement.

LINEAR SYSTEM ANALYSIS

The principal motivation for developing the SAND system was to use all of the available "information" in an active neutron assay. Existing active prompt fission neutron systems may only count for a fraction of the interrogate-count cycle. We felt that to exploit the unique features of the Schlumberger neutron generator and also use all of the available information required a formal analysis using linear system theory. Establishing that the active neutron system was in fact linear was the first part of the experimental schedule.

Linear theory is a mature and comprehensive technique that allows analyzing systems from two equivalent viewpoints: the time domain and the frequency domain. The conversion from one domain to the other is done by Laplace and Fourier transforms. Often, systems that seem complicated in the time domain appear understandable in the frequency domain. The SAND concept evolved from the frequency domain analysis of an active neutron assay system.[2,3]

For example, Fig. 2 illustrates two of the important features of linear systems. These are as follows:

1. The response of a linear system to an impulse function is equal to the system function of the system. This case is unique; all other driving functions must be convolved with the response function. For example, the simple system depicted in Fig. 2 responds to an impulse with a decaying exponential. Thus, the system function is a decaying exponential, which can also be expressed in the frequency domain as the algebraic function $1/(s + a)$. The significance in this instance is that it becomes possible with the neutron generator to measure the system function of the neutron assay system. The neutron generator is programmed to produce a short impulse of neutrons. The resulting neutron count rate as a function of time is the system function of the system.

2. Any complex exponential, therefore any sine wave, is an eigenfunction of a linear system. The significance of this feature is that when a linear system is driven by a sine wave, it will respond with the same sine wave, modified only in amplitude and phase. The input and output frequencies will be identical. Equivalently, the complex exponential eigenfunction is multiplied by a complex eigenvalue.

This second feature and a simple trigonometric identity provide the basis for synchronous detection, illustrated in Fig. 3. When the product of two sine waves is integrated over time, the integral is zero except when the frequencies are identical.

$$\int_{-\infty}^{\infty} dt\, e^{i(\omega_1 t+\phi_1)} * e^{i(\omega_2 t+\phi_2)} = \delta(\omega_1-\omega_2) * \cos(\phi_1-\phi_2) \qquad (1)$$

and equivalently in discrete time :

$$\sum_{n=1}^{N} \sin(\omega_1 n-\phi_1) * \sin(\omega_2 n-\phi_2) = \delta(\omega_1-\omega_2) * \cos(\phi_1-\phi_2)$$

$$\text{for } N \rightarrow \infty$$

Equation 1 enables selecting, or projecting out, a single Fourier component of a complicated signal. A linear system driven by a sine wave responds with the same sine wave modified only in amplitude and phase. Therefore, to measure the response of a linear system, we drive it by a sine wave. The output will be a sine wave of the same frequency but presumably mixed with noise and interference. The output is analyzed by Eq. 1, using the input as the reference. The result will be the system response at this frequency because only the one frequency component corresponding to the driving source will survive. All other Fourier components of the output, due to noise or interference, for example, are eliminated.

This process is the basis for synchronous detection. A reference signal is generated that is used to drive a linear system. The response of the system is then multiplied by the reference signal (suitably phase-shifted) and the product is time integrated. The result is the system response at that frequency. All other noise and interference components not of the proper frequency and phase are filtered out. Only noise that matches the precise frequency and phase survives, and this can be a very small fraction of the total interference. Typical, commercial lock-in amplifiers that implement the synchronous detection technique resolve signals at 10^{-8} compared to the noise.[4]

Figure 3 illustrates the benefit of synchronous detection for the active neutron assay application. If an assay system were driven by a pure sine wave, the response would be a sine wave with the same frequency but perhaps a different phase. This sine wave would be the single Fourier component that would survive the synchronous detection filter. All of the system response to the neutron interrogation would be measured. By contrast, the ambient passive neutron signal obeys the normal distribution (for large counts). The time series for the ambient count rate will be a normal distribution about a mean value. The spectral density of this time series will consist of a large zero frequency, dc, component corresponding to the mean value, and a flat spectrum corresponding to the fluctuations.

In the discrete time domain, the broad, flat portion of the spectrum corresponding to the fluctuation level will have an amplitude equal to the variance of the ambient neutron count rate divided by the number of bins. Because the synchronous detection filter selects only a single bin, only one bin's worth of noise survives. The rest are eliminated. The effect of the noise is reduced by the number of time or frequency bins.

The overall improvement in background reduction can be expressed in terms of the number of "noise bins." In discrete time, the Fourier transform converts a time series into a frequency representation. The number of frequency bins is identical to the number of time bins. Therefore, a single frequency bin of noise is equivalent to a single time bin of noise. The background rejection improvement can be thought of as reducing the count time to a single time bin (with all the desired signal surviving).

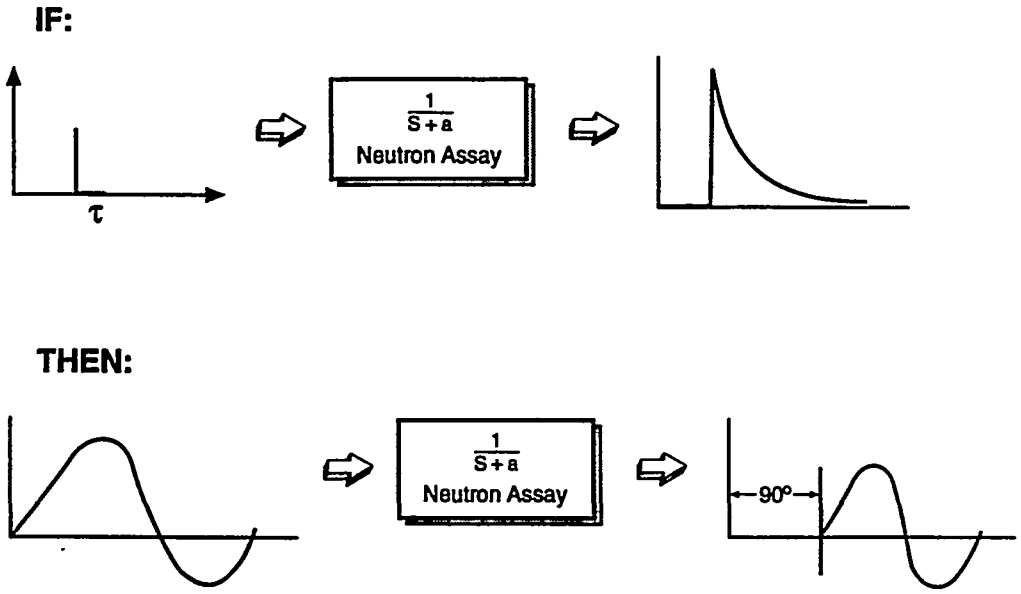

Fig. 2. This diagram illustrates some of the basic principles of linear systems. At the top, a linear system excited by an impulse responds with the system function. For the decaying exponential shown, the frequency response of this system to a sine wave is a sine wave at the same frequency but at a different phase and magnitude. For frequencies above the inverse decay time pole, the phase delay is 90 degrees. The system function for this example is shown in the diagram and is a simple pole.

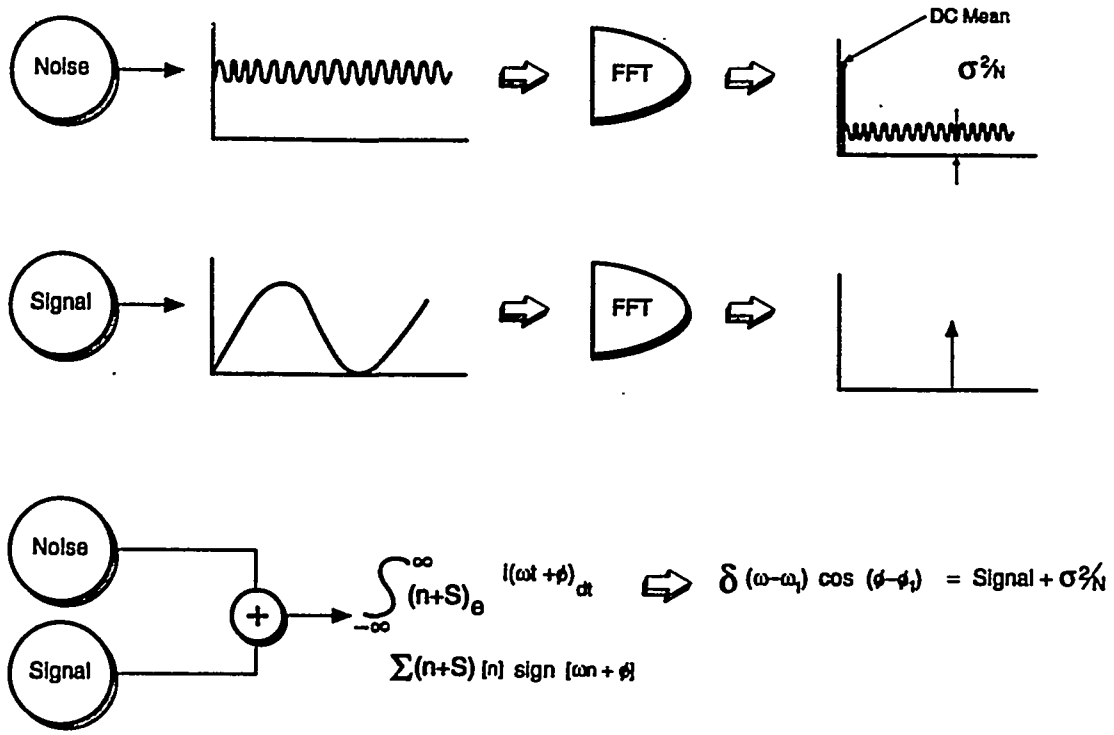

Fig. 3. This diagram illustrates some of the potential benefits of linear system theory for this application. At the top, a typical neutron signal represented as white noise is Fourier transformed. The result is that the variance of the noise is divided by the N *frequency bins of the discrete Fourier transform. However, as shown at the bottom, the Fourier transform of a sine wave appears in only one frequency bin. Systems excited by a sine wave therefore recover all of the driving term but only a small fraction of the background noise. The method for projecting out the sine wave component is the time integral shown at the bottom.*

EXPERIMENTAL APPARATUS

A schematic of the neutron generator, data acquisition system, and control system is shown in Fig. 4. The entire control and data acquisition system is computer-software controlled. The major components of the system are as follows:

1. The PC-based computer with attached PC-bus expansion chassis to accommodate additional interface boards.

2. The Schlumberger neutron generator tube, which is enclosed in a pressure chamber for high-voltage stand-off. A neutron scintillation detector is mounted adjacent to the generator tube to monitor 14-MeV neutron output.[1]

3. The power and control electronics for the Schlumberger neutron generator. Three separate circuits are energized to operate the tube: the high ion accelerator voltage that accelerates the deuterium and tritium ions to collide, an intermediate voltage that creates the source plasma, and a current source used to heat the source filament/getter that controls the plasma density, the beam current, and the neutron yield. The control electronics contains a feedback system that controls the filament current to maintain a constant beam current in the accelerator portion of the tube. (The beam current is measured as the current drain on the high-voltage supply). The generator tube output is switched by switching the intermediate (2.2 kV) supply. A digital waveform generator board in the PC expansion chassis provides the TTL-compatible signal to control the switching. Therefore, the computer system can program the neutron output waveform in both frequency and duty factor.

4. The assay chamber consists of the neutron generator, neutron monitor, ^{3}He neutron detector tubes embedded in polyethylene, the cold fuel sample, and surrounding walls of cadmium-covered polyethylene. The chamber geometry is shown in Fig. 5.

5. Amplifier electronics for both the scintillator and the ^{3}He detector signals.

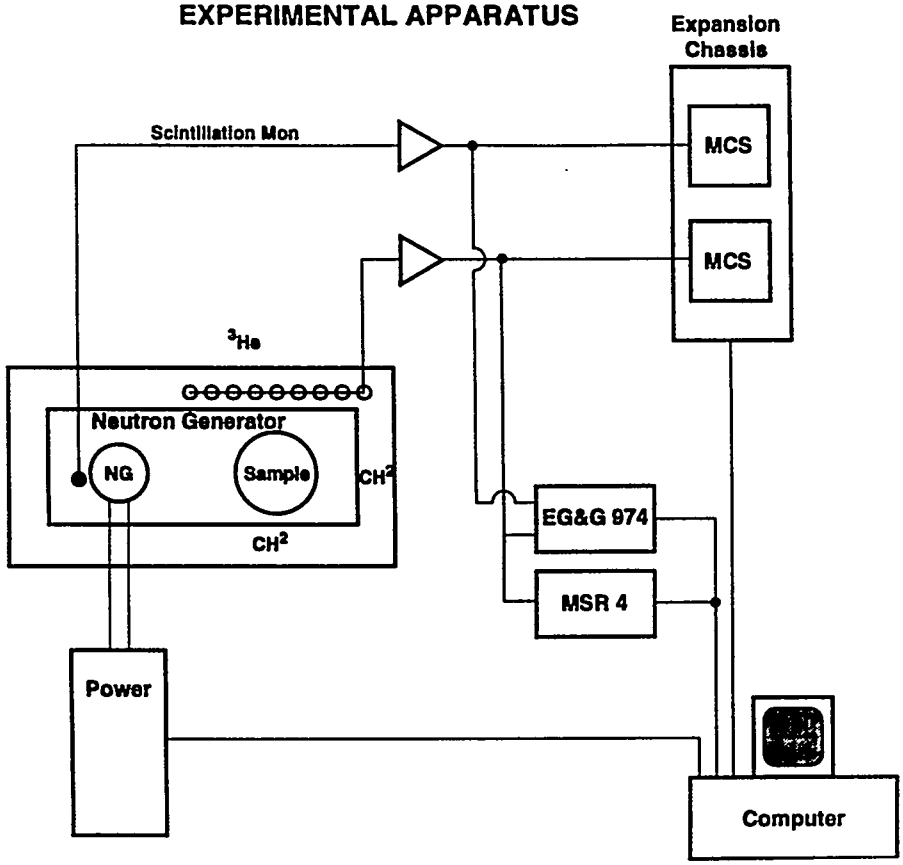

Fig. 4. A schematic of the control system for the neutron generator and the data acquisition system.

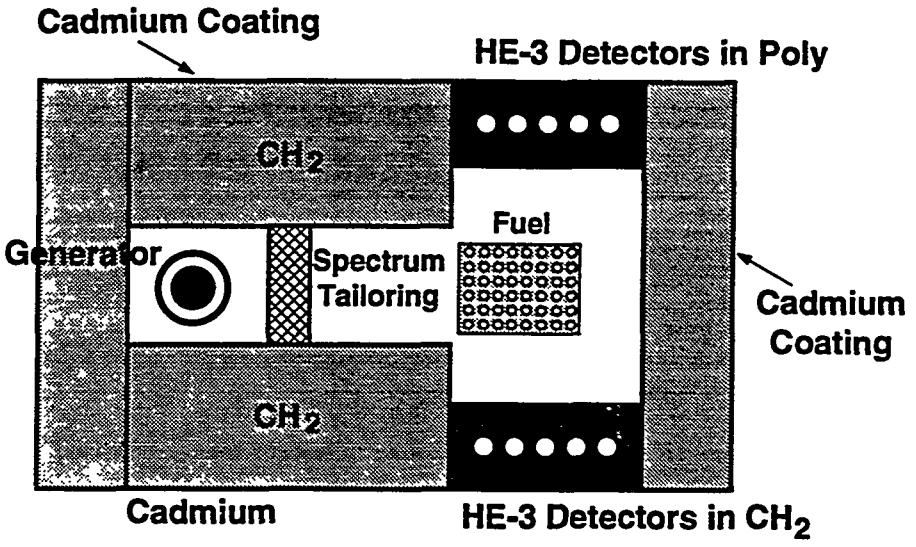

Fig. 5. A diagram of the assay chamber geometry showing the neutron generator, neutron monitor, the fresh fuel assembly, and the ^3He detectors embedded in polyethylene. Note that the chamber walls are cadmium-covered polyethylene to shield the detectors from the interrogating neutrons and to maintain a "hot" interrogating spectrum.

6. An EG&G Model 974™ quad counter and an MSR-4 multiplicity counter. The gating for these counters is controlled by an interface board in the expansion chassis and is programmable from the operating software. Any gating window can be selected. The quad counter counts the neutrons in the specified gate from both the scintillator and the ^3He detectors.

7. A PC expansion chassis that contains digital interface boards. These I/O boards monitor and control the Schlumberger control electronics and provide the waveform for neutron pulsing. All control aspects of the neutron generator are under software/computer control.

8. Two EG&G ACE-MCS™ multichannel time scaler boards in the expansion chassis, under software control.[28] One board measures the neutron count rate of the scintillation detector and the other measures the count rate of the ^3He detectors. These boards are multichannel time scalers; they count pulses in successive time bins. During each bin time, the board counts neutron pulses digitally, then sequences to the next bin. The number of bins and the time-width of the bins is programmable and can vary from 4 to 4096 bins and from 2 μs in width to 35.7 min. These boards enable the measurement of the time behavior of the neutron count rate. Typically, we operated with 128 time bins that were 3 μs wide for both boards.[28]

The multichannel time scalers are a particularly important feature of this system. These boards count neutron pulses in many (~128), small (~3 μs) time bins. They provide a well-resolved, discrete-time history of the neutron count rate. Therefore, the time response of the neutron assay system can be measured. All plots in this paper of neutron count rates vs time are plots of the neutrons counted in these time bins.

The entire system was operated from the computer and could be easily programmed to any desired configuration. Adjustable parameters included the frequency and duty factor for the neutron pulses, the number of neutron pulses for a single data run, the gated on and off times for both the EG&G 974 and the MSR-4 counters, and the number and width of the time bins in the ACE-MCS multichannel scalers.

A detail of the assay chamber is shown in Fig. 5. The chamber was designed to insure that the interrogating neutron spectrum was energetic and penetrating. The 14-MeV neutrons are slightly moderated by a 0.5-in.-thick sheet of polyethylene. We are currently exploring other options to improve the spectrum tailoring. The chamber is entirely covered with 0.03-in.-thick cadmium to prevent thermal neutrons from the polyethylene walls from re-entering the chamber.

Interrogating Energy Spectrum

We have examined the issue of whether the interrogating neutron spectrum was sufficiently energetic to penetrate and evenly sample the fuel rod assembly. MCNP calculations were done to model the entire detection system.[29] Some of these results are shown in Fig. 6. Two MCNP tallies were made: one was the energy distribution of the neutrons leaving the spectrum-tailoring material, and the other was the spatial distribution of induced fissions in the fuel assembly. The interrogating neutron energy spectrum is broad and extends up to the 14-MeV source level. There does not appear to be a large concentration of thermal neutrons. This spectrum is highly penetrating and should sample the fuel assembly somewhat evenly, although some neutrons will equilibrate with the polyethylene wall. The more direct measure of the sampling effectiveness of the interrogating neutrons is shown in the bottom plot of Fig. 6, which shows the normalized distribution of induced fissions as a function of fuel rod row, measured from the front surface. The decay of the induced fission rate is gradual and the entire assembly is sampled.

The assay data of the fuel rod assembly is another indicator that the interrogating neutrons are effectively sampling the assembly. The sensitivity of the measurement to individual fuel rods seemed largely independent of position. These results will be discussed in greater detail in a later section.

In this configuration there is negligible phase (or time) delay between the interrogating and induced fission signals. The reason is that the equilibration time (time to become thermalized) for neutrons is very short compared to the period of the interrogating waveform. To see a phase shift under these conditions, the neutron pulse frequency f would have to be much greater than the pole at the inverse equilibration time:

$$2\pi f >> \frac{1}{\tau_E} \qquad (2)$$

For nominal thermalization times of $\tau_E \simeq 3\ \mu s$, the interrogating frequency would have to be larger than 53 kHz, well above the operating range of the neutron generator.

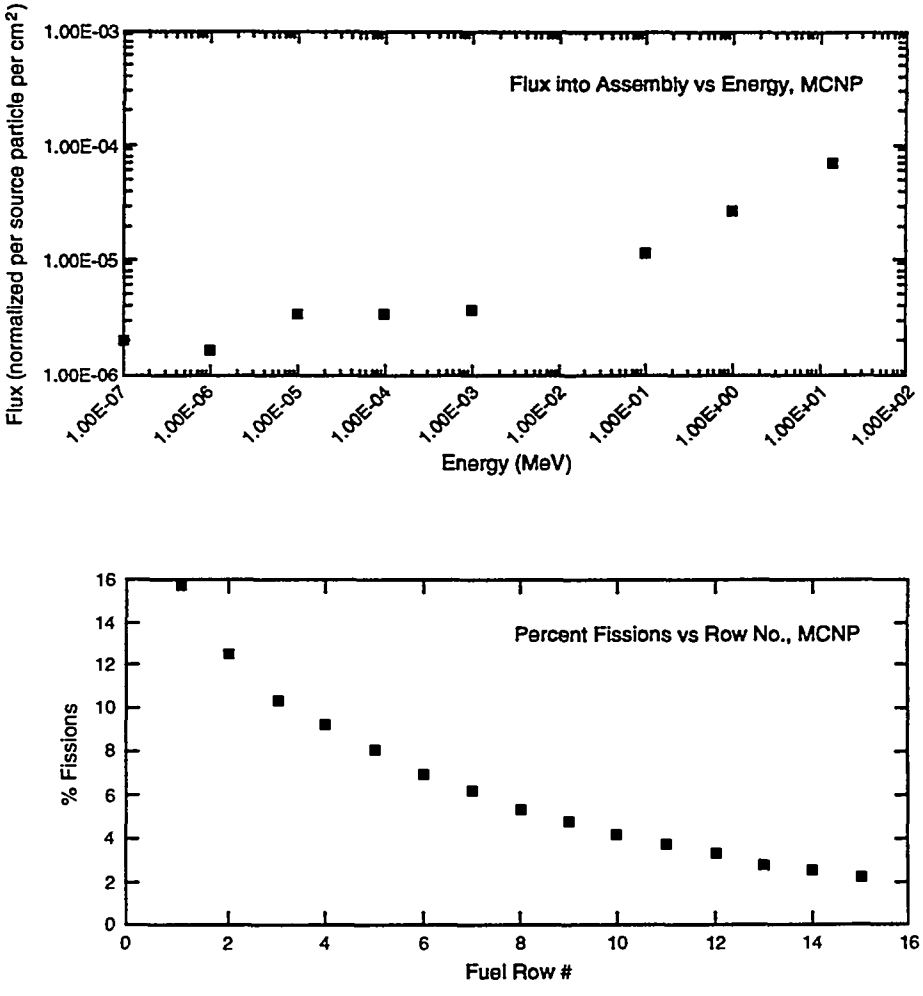

Fig. 6. Results of MCNP modeling of the assay chamber. The top plot shows the energy distribution of the neutrons leaving the spectrum tailoring material. Note that the energies are broadly distributed at high values, up to the 14-MeV source level. The bottom plot shows the distribution of fissions inside the spent fuel assembly, as a function of fuel rod row measured from the first row. Note that the decay in the induced fission rate is gradual and the entire assembly is sampled.

Because the interrogating neutron counts cannot be separated from the induced fission neutron counts using a phase difference, the separation is largely accomplished by exploiting the assay chamber geometry. The ^{3}He detectors are shielded from direct exposure to the neutron generator and the spectrum tailoring material. Detected neutrons must be either fission neutrons from the fuel assembly or scattered interrogating neutrons. The cadmium-coated chamber should reduce much of the scattered signal. Preliminary results show that the ratio of detected fission neutrons to interrogating neutrons is about 0.4. No chamber optimization was done prior to this measurement. Future work will explore design modifications to reduce the scattered component and improve this ratio.

EXPERIMENTAL RESULTS

Basic Response Tests

Impulse Test

Because the method of synchronous detection is quite novel for active neutron assay, the fundamental operation and physics of this system was investigated before attempting an actual assay. The first step toward characterizing this system was to determine the impulse response. The impulse response is fundamental to a linear system because it defines the system function. The presumption for our development was that the impulse response for this assay system would be a simple decaying exponential, which is how neutrons are expected to die away in active neutron assay chambers.

To test this assumption, the neutron generator system was programmed to produce the shortest neutron pulse possible, about 15 μs long. The initial pulse waveform and magnitude was monitored using the scintillation detector and one of the ACE-MCS scaler boards. The response of the ^{3}He detector tubes was also measured using the second multichannel time scaler. Both boards were programmed for 100 bins, each 5 μs wide. The results are shown in Fig. 1.

The plots in Fig. 1 show the time history of the neutron generator pulse and the detection system response. To achieve acceptable statistics, we measured 20 000 pulses and the counts were accumulated in each time bin. The timing for the multichannel scaler was established using the leading edge of the neutron generator pulse as a time fiducial.

The waveform of the ^{3}He-detected neutrons appears approximately, but not exactly, as a decaying exponential. However, attempting to fit this curve to a decaying exponential is not adequate because the neutron generator pulse was not an ideal delta function in time. To properly analyze the system response, the finite width of the initial pulse must be deconvolved with the measured response.

The deconvolution procedure can be made relatively easy by using Laplace transforms. The Laplace transform of the finite-width neutron generator pulse was modeled using terms in the form e^{-sT}/s, where s is the Laplace complex frequency variable and T is the time delay or pulse width. The inverse Laplace transform of this model is fitted to the data. Then this fitted Laplace model was multiplied by terms of the form $1/(s + a)$, which correspond to the decaying exponentials: $e^{-a\tau}$. The inverse transform of this combined model was then fitted to the ^{3}He data by adjusting only the parameters for the decaying exponentials. The result is a complete model and the model parameters specify the exponential decay time. The model fits to both the generator pulse and the detected neutrons, and the exact model equations are shown in Fig. 7.

These results show that the dominant system response was a decaying exponential with a decay time of 131.5 μs. The frequency domain representation is $H(s)=1/(s + a)$, where $(s + a)$ is the simple pole corresponding to the inverse decay time.

There was also a second exponential detected at roughly 13 μs.

Linearity Test

The next test for this system was to further establish linear behavior. A linear system must satisfy only two essential conditions: time invariance and superposition. Because there are no physical changes to the assay system, time invariance is satisfied. Superposition will be generally satisfied because neutrons do not interact with one another. An exception would be the saturation of the neutron detectors or detector electronics. Saturation is a concern because it occurs when the generator produces high-yield, narrow neutron pulses. To establish that saturation does not occur when operating in the square wave mode, we compared the measured output from the assay chamber ^{3}He detectors to the output from the scintillation detector, which monitors the neutron generator yield.

The neutron generator was programmed to operate at a 50% duty factor (square wave) at a pulse frequency of 2.6 kHz. Both the scintillation neutron monitor and the ^{3}He-detector outputs were measured using the multichannel scaler boards. The yield of the neutron generator was then scaled by adjusting the accelerating high voltage from 10 kV to 90 kV in 10 kV steps. Typical data from the neutron detectors are plotted in Fig. 8.

At each point, the time-integrated, total neutron generator output (scintillator) and ^{3}He-detected neutrons were measured. The results are plotted in Fig. 9. The plot of the detector response as a function of neutron generator yield in Fig. 9 shows a linear response up to the highest voltage settings and neutron output. This test confirms that the detectors are not saturating and that the system is operating in a linear mode.

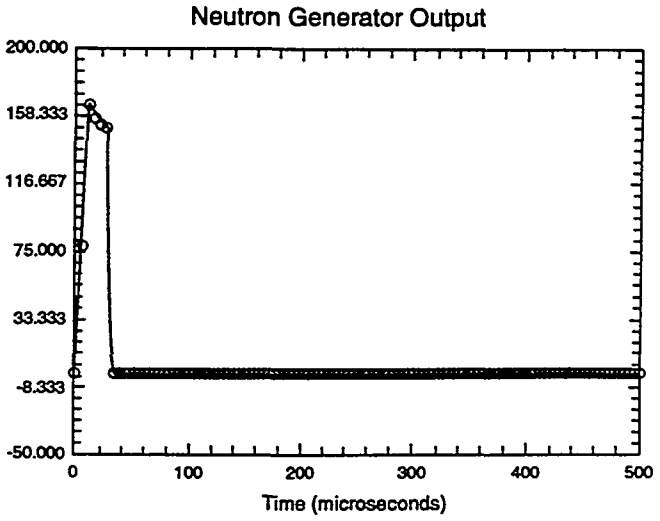

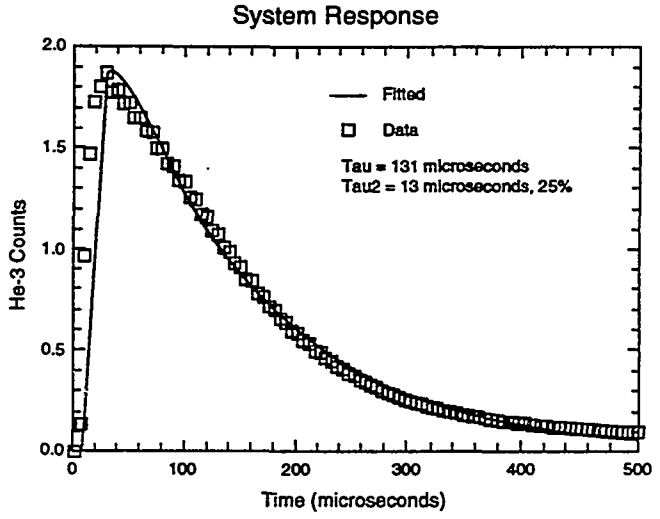

Fig. 7. Laplace transform models fitted to the neutron generator pulse and the resulting detected neutron waveform. The model equations are also shown.

$$s = p\,[\exp(-s\tau_1) + \beta \exp(-s\tau_2)$$

$$S = \int_{-\infty}^{\infty} d\tau\; p(t-\tau)\,[\exp(-t/\tau_1) + \beta \exp(-t/\tau_1)]$$

Deconvolution Technique

To further explore and confirm the linear operation of the assay system, we investigated the response of the system in the frequency domain. The first test was to experimentally measure the actual phase shift of the interrogating neutron waveform. The method for digital deconvolution of the neutron count rate follows closely the methods used by commercial lock-in amplifiers. Figure 10 plots the rate of detected neutrons by the assay chamber as a function of time. This time series is a nominal, detected-neutron time series in the synchronous mode. The procedure for implementing synchronous detection on this data is to calculate the time integral (sum in discrete time) of the product of the time series with the interrogating neutron sine wave (appropriately phase shifted). The formula for this calculation in discrete time is

$$R(\phi) = \sum_{n=1}^{N} x(n) * \sin(\omega n - \phi) \qquad (3)$$

Equation 3 selects the single Fourier component of $x(n)$ with the same frequency and phase as $\sin(n - \phi)$. All other frequencies are eliminated and other phases are attenuated by the cosine of the angle difference, according to the equation

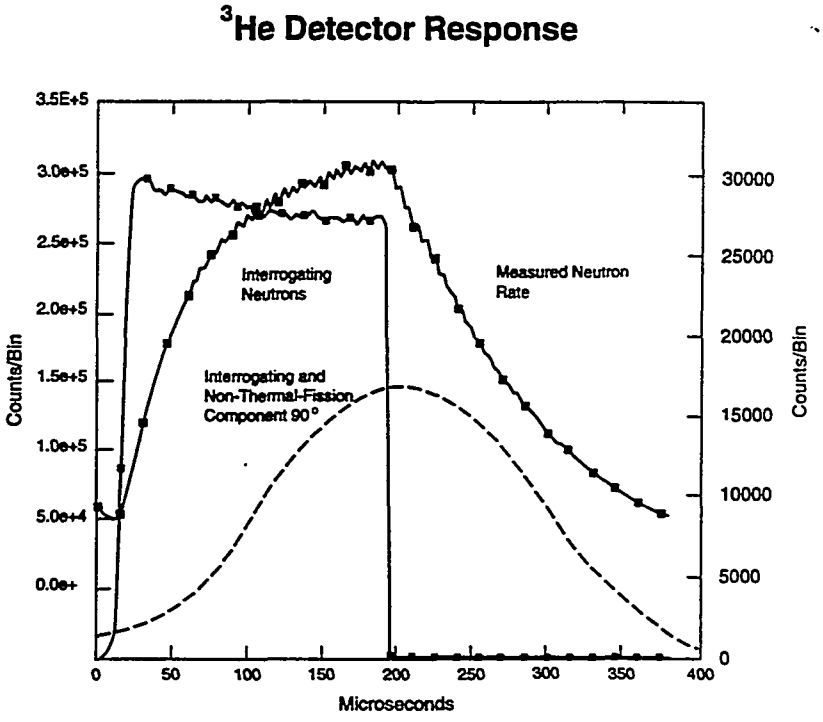

Fig. 8. Plot of the ^{3}He accumulated counts as a function of time for a square wave neutron output. This is the nominal response of the system when measuring the fuel assembly. Also plotted are the assumed ideal phase shifts expected for operation at frequencies well above the inverse die-away time. The 90 degree phase shift corresponds to the interrogating spectrum and fissions induced from nonthermal neutrons. The 180 degree phase shift would be expected from thermal neutron interrogation.

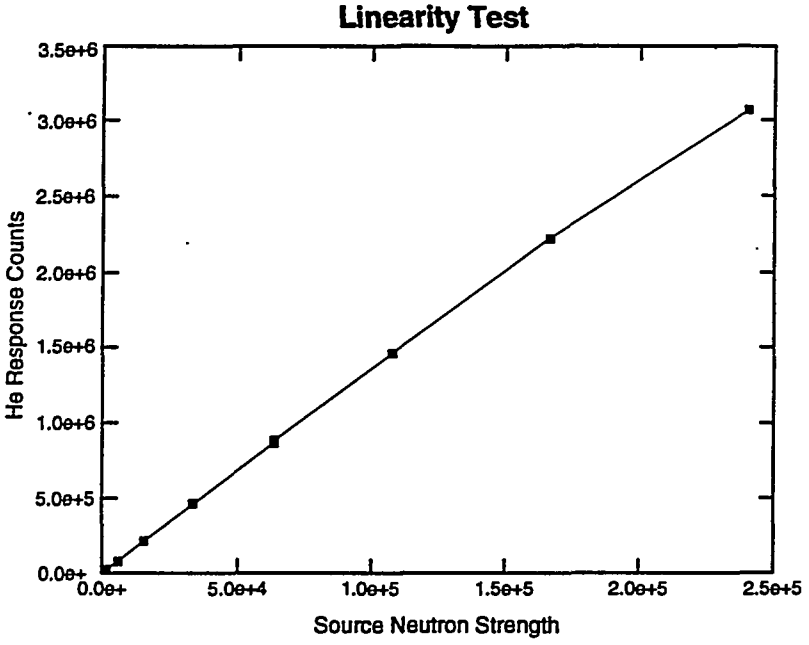

Fig. 9. Detected neutrons as a function of the neutron generator output, operating in the 50% duty factor mode. Note that the response is completely linear.

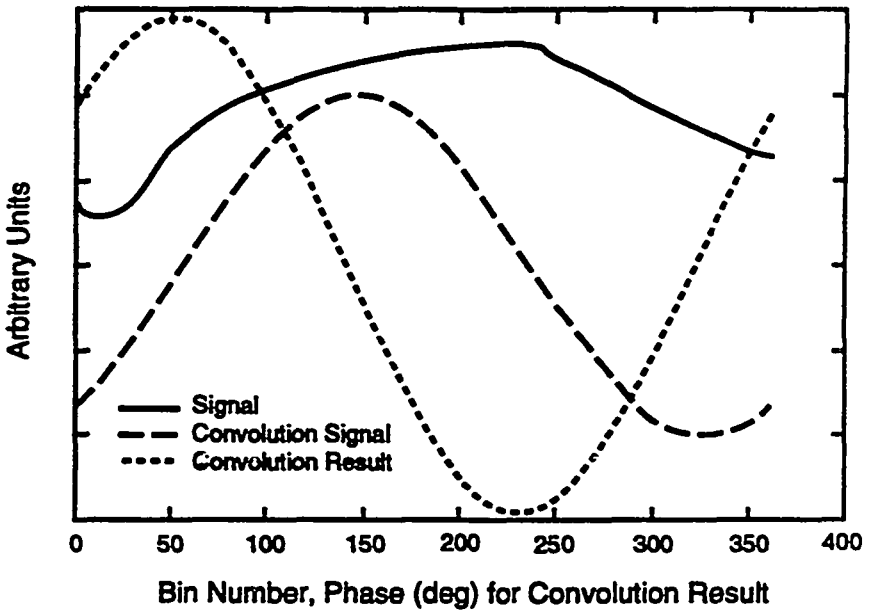

Fig. 10. This plot shows a nominal measured neutron pulse in the square wave mode. Also shown is the optimal sine wave for time integration. Finally, the time integral as a function of the phase shift is plotted. The optimum phase shift for this particular data set is about 50 degrees.

$$\sum_{n=1}^{N} \sin(\omega_1 n - \phi_1) * \sin(\omega_2 n - \phi_2) = \delta(\omega_1 - \omega_2) * \cos(\phi_1 - \phi_2) \qquad (4)$$

For a lock-in amplifier, the condition that the reference frequency, ω_1, matches the desired system response frequency, ω_2, is guaranteed because the system response frequency is identical to the driving frequency.

The procedure for implementing synchronous detection digitally for this application follows the method used by modern lock-in amplifiers.[4] The leading edge of the neutron square wave is used as a time fiducial. The data analysis software generates a synthetic sine wave synchronized with this leading edge. The synthetic sine wave is appropriately phase shifted and becomes the reference signal. It is time integrated with the detected system response to extract the desired Fourier frequency and phase component.

However, there are two considerations for a lock-in amplifier (Eqs. 3 and 4) in this particular instance. The first consideration is due to the square wave interrogating waveform. In an ideal lock-in amplifier system, the interrogating (reference) waveform is a sine wave. For this active neutron assay system, however, the interrogating waveform is a neutron square wave. This effect of using a square wave is to introduce Fourier components at the even harmonics of the square wave frequency. No error is introduced because these harmonics are suppressed by the lock in system. However, some of the sensitivity is lost because not all of the neutron signal is concentrated in the fundamental sine wave.

The second issue is the selection of the proper phase delay of the reference signal to match the real phase shift of the measured neutron signal. Optimally, these two phase delays should be the same to obtain the most sensitive response based on equation 4: cos(0)=1.

The selection of the proper phase shift for the reference signal delay had to be done experimentally. The method is illustrated in Fig. 10. Figure 10 plots the time series of the measured neutron rate and the sine wave with "optimal" phase shift. The optimal phase shift was determined by calculating the time integral of the product between the data and the synthetic reference as a function of phase shift. That is, Eq. 3 was calculated for the entire range of possible phase shifts: $0 \leq \phi \leq 2\pi$. These results are also plotted in Fig. 10. These results follow the expected cosine dependence of Eq. 4. The peak of this plot corresponds to the point of zero phase difference: the ideal phase shift. As the phase shift changes from the ideal, the value for the time integral, Eq. 3, decreases as the cosine. Therefore, the proper value for the phase shift is simply the phase value corresponding to the peak shown in Fig. 10. The resulting cosine curve corresponding to this phase shift is also plotted in Fig. 10.

Most of the data taken in these investigations were at an interrogating frequency of 2.6 kHz. The corresponding optimal phase shift is 59 degrees. This value of ϕ should be in phase with the prompt fission neutron signal induced by the "hot" neutrons. The reason

is that the neutron thermalization time τ_T is quite short in most materials, on the order of just a few μs. Because the operating frequency $\omega = 2\pi f$, where $f \cong 2.6$ kHz and $\omega \cong 1.6 \bullet 10^4$ rps, is too low compared to the frequency corresponding to the thermalization time ($s = 1/\tau_T = 1/3 \bullet 10^{-6}$, $s \cong 3.3 \bullet 10^5$) there is no additional phase shift from the thermal neutrons.

Phase Test

We conducted another test to establish that this system is linear and that the system function is a simple decaying exponential. A simple decaying exponential in the time domain corresponds to a single pole in the frequency domain. For interrogating frequencies well below the pole frequency, there should be no phase shift. For frequencies well above the pole frequency, there should be a phase delay of 90 degrees. For frequencies close to the pole frequency, the phase delay should increase monotonically with frequency from zero to 90 degrees.

We tested this behavior by scaling the neutron generator over the full range of allowed frequencies for a 50% duty factor, 2 kHz $\leq f \leq$ 3 kHz, and measured the "optimum" phase shift. The results are plotted in Fig. 11. As expected, the optimum phase shift increases monotonically with frequency. Quantitatively, the phase shift matches the expected value for a single pole at $s = 1/\tau_D, f = 1/2\pi\tau_D$, where $\tau_D \approx 105$ μs and $f \cong$ 1515 Hz. This value is a slight departure from the nominal die away time of 131 μs measured in the time-domain. However, the Laplace transform analysis also revealed a second smaller pole at 13 μs. The combined effect of both poles is certainly consistent with the measured phase delay shown in Fig. 10. Therefore, the behavior of the system is consistent between the time and frequency domains.

NOISE REJECTION TEST

The next test investigated whether the synchronous detection method is more resilient to the ambient neutron interference than conventional background subtraction methods. This issue was tested by comparing two methods for separating the background neutron rate from the desired signal. Because the issue is strictly background elimination, we compared two systems for removing the background neutron interference from a measurement of the neutron generator signal. The methods were synchronous detection and conventional background subtraction. These tests repeated the output scaling measurements for the linearity test above, with several important differences. First, the measurements were conducted using an intense ^{252}Cf source to provide the ambient neutron background. Second, two sets of measurements were made: one using synchronous detection and generating a square wave neutron output, and the other using conventional background subtraction and producing narrow neutron pulses, as is done conventionally. In both cases, the total neutron output was the same. The accelerating voltage, neutron output rate, and total assay time were kept identical between the two sets of measurements. For the short-pulse measurements, a background count was done as well.

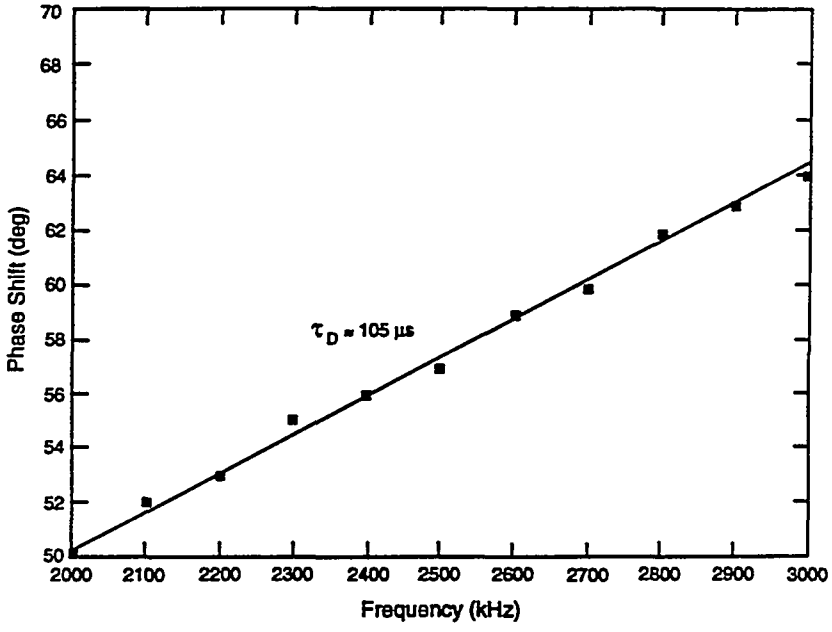

Fig. 11. A plot of the phase delay of the fundamental of the neutron generator waveform as a function of pulse frequency. The monotonic increase in phase delay over this frequency range confirms the linear behavior of the system and the single pole at the inverse die-away time.

These measurements were also done at a much lower accelerating voltage and neutron yield than for the linearity test. The accelerating voltage was scaled from 10 kV to 35 kV only. The neutron yield at 35 kV is over one order of magnitude lower than at the maximum 100 kV level. The lower neutron yield was necessary to effectively increase the effect of the ambient neutron source (the significant effect is the ratio of the background source strength to the neutron generator source strength). The second reason was to prevent detector saturation when running in the "short pulse" mode.

A final condition was that the measurements were conducted for 50 000 neutron pulses to obtain sufficient counting statistics. The fluctuations in the measured data reflect the interference of the ambient background neutrons, not any lack of statistical precision. The variance of the data from counting statistics was determined to be two orders of magnitude less than the observed variance.

Both the synchronous detection and conventional subtraction results are plotted in Fig. 12. At each of several accelerating voltages, several measurements were made to determine repeatability and precision. In both cases the mean response of the system scales quite linearly with the neutron generator source strength. However, there is considerably more scatter in the conventional data than for the synchronous detection data. The only difference between the two data sets is the method for extracting the neutron generator data. The important observation from these tests is that the relative variance of the synchronous detection data is a factor of 4 better than for the conventional case.

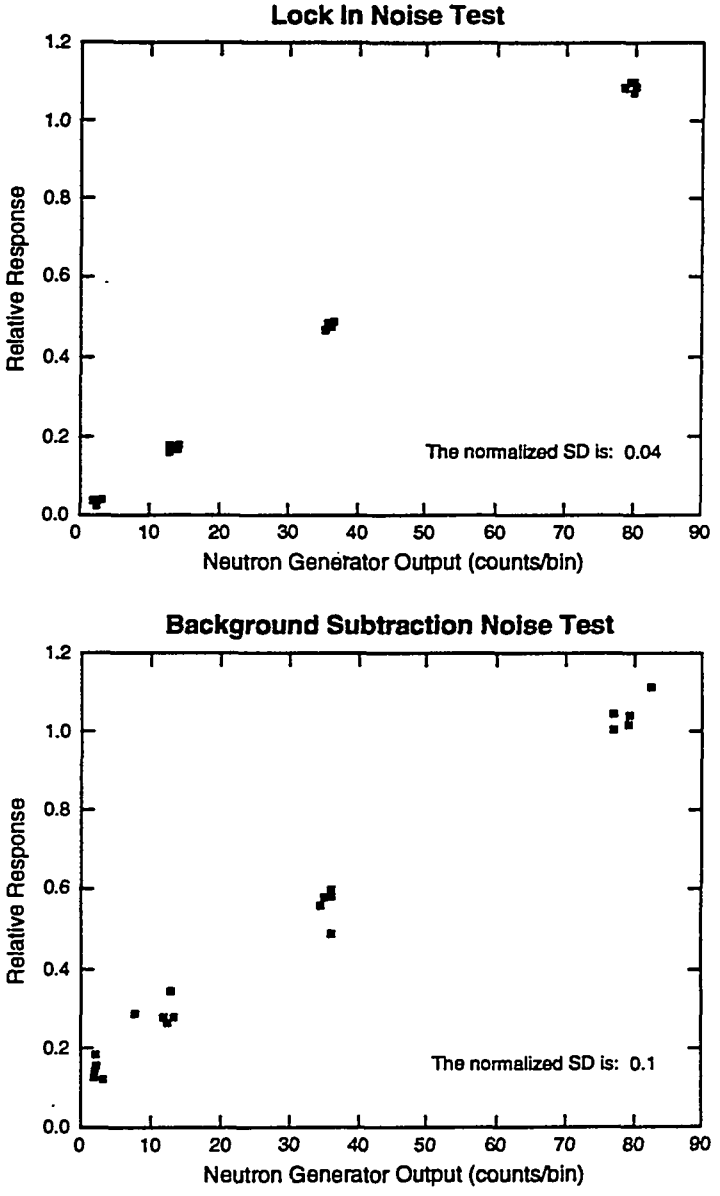

Fig. 12 Plots of the relative response of the detection system to equal neutron interrogation fluxes. In both cases the relative response is plotted against the neutron generator output. One method uses synchronous detection to separate the neutron generator signal from the ambient background; the other method uses conventional background subtraction. Note that both measurements scale linearly with source strength as expected. However, there is much less scatter in the synchronous detection data than for conventional background subtraction.

Therefore, the synchronous detection method is measurably more resistant to interference from ambient background neutrons.

COLD FUEL MEASUREMENTS

The final test for these preliminary investigations was to determine whether the SAND system could accurately and reliably measure fissile material in a fresh fuel assembly. For these tests we measured the output of the SAND system as a function of the number of fuel rods in a fuel assembly. The measurement was repeated several times for different amounts of fuel rods present in the assembly. We did not attempt to absolutely calibrate the system, rather, the intent was to determine the measurement resolution in terms of the number of rods that could be resolved in the assembly.

The rods were also added and removed from different locations in the fuel assembly, to test the uniformity of the spatial response. Although the spatial uniformity was not measured in a detailed fashion, selecting different locations would presumably increase the overall data scatter.

The SAND system was operated at a frequency of 2.6 kHz, a duty factor of 50% (for synchronous detection), and 500 000 neutron pulses were done for each data point. The average assay took roughly 5 min to complete. The multichannel scalers were programmed for 128 bins of 3 μs each, for both the neutron monitor and the ^{3}He detected neutrons. Nominal data are shown in Fig. 13 for the extreme cases of an empty fuel assembly and a full fuel assembly. The interrogating neutron pulse is also plotted.

The fuel assembly itself can hold a maximum of 204 fuel rods in a 15 by 15 matrix. Each fuel rod is stainless-steel-coated uranium oxide at 3.19% enrichment. Each rod contains 19.75 grams of ^{235}U.

The detection chamber design was not optimized for these tests. The nominal neutron detection efficiency was roughly 3% and the die-away time was 130 μs. The floor of the chamber was cadmium-coated concrete. The top of the assay chamber was open.

A total of 27 data points were taken for this initial test. The results are plotted in Fig. 14, which shows the total synchronous detection counts normalized to the number of bins, as a function of the number of fuel rods in the assembly. Because a significant signal is present without fuel rods present, the data are normalized by subtracting the zero fuel case. The data in Fig. 14 demonstrate a very linear response of the SAND system to the amount of fissile material present. Moreover, the different spatial positions of the rods that were removed do not seem to have significantly degraded the results.

An exploded view of these data is shown in Fig. 15, which plots only the cluster of data near a full fuel assembly. A total of 14 data points are plotted. This plot shows the response of the system when only a few rods are removed from a full fuel assembly and measures the resolution of this configuration. From these data, the SAND system can resolve 10 fuel rods in a fuel assembly of 204, which satisfies the IAEA fiducial of 10% resolution.

CONCLUSIONS AND REMAINING WORK

There are several conclusions and clear directions for future research from this work:

1. The SAND system is capable of measuring the fissile material in cold fuel with acceptable precision at present. The resolution of the measurement was about 10 rods in a fuel assembly consisting of 204 rods. The IAEA safeguards fiducial for spent fuel is the detection of 10% of the fuel rods, which would be 20 rods in this instance. In addition, the detection chamber design has not been optimized. The detection efficiency is roughly 3% and much of the geometry is open. The spectrum tailoring material has not been optimized and the geometry has not been optimized to improve the ratio of fission neutrons to interrogating neutrons. Finally, experiments with interrogating frequency will be conducted to determine the optimum neutron pulse frequency. At present, only a partial phase shift is achieved. A more complete phase shift of 90 degrees might improve performance. With these improvements, the measurement precision could be improved.

2. The synchronous detection method appears to be more resilient to background (neutron counting) interference than other techniques. We presented data comparing the SAND method to conventional background subtraction using a pulsed neutron source, and the variance for synchronous detection was less by a factor of 4. Moreover, the SAND method measures prompt fission neutrons, so it would probably have a natural advantage compared to delayed neutron interrogation methods. Other spent fuel measurement techniques, such as the active neutron collar, are also not resilient to background neutron interference.

3. Although the SAND approach shows promise in this area, a detailed comparison of the noise immunity of synchronous detection is one of the areas for future research. The noise immunity of the SAND system has not been tested at the extreme required for the spent fuel measurement. We plan to repeat the cold fuel assay measurements using the californium source and a reduced neutron generator yield, as a next step.

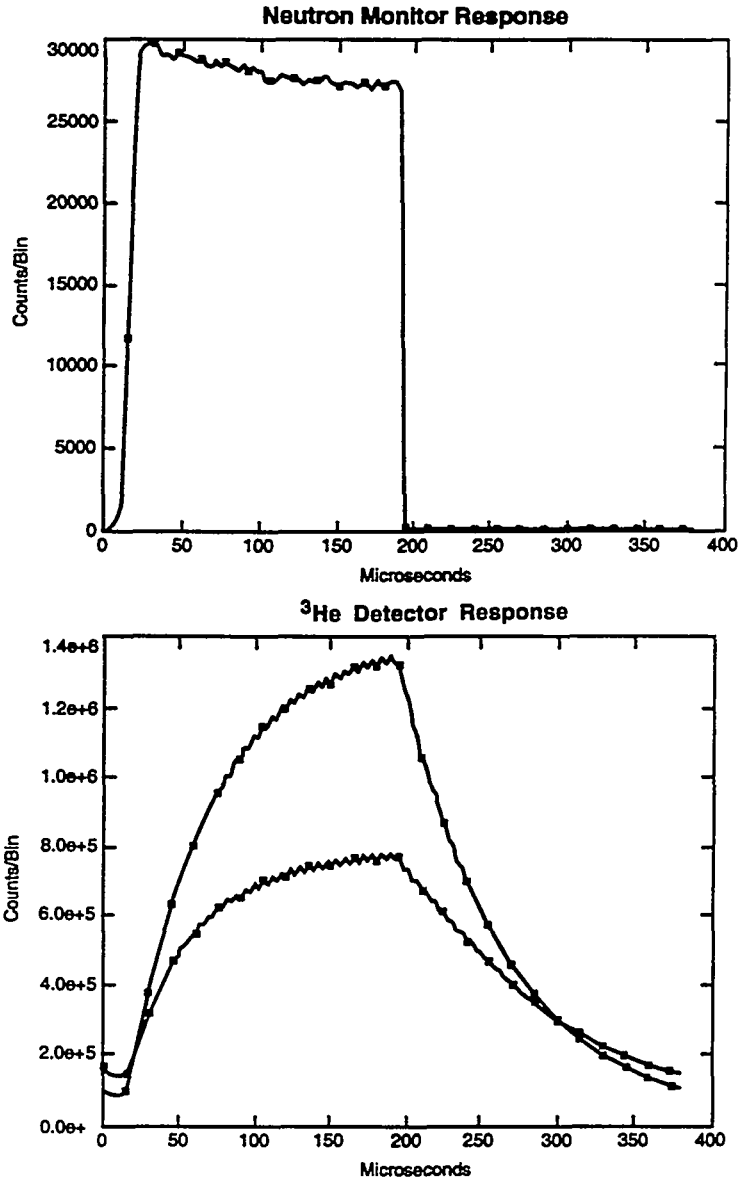

Fig 13. Plot of the interrogating neutron pulse and the assay system response for two cases: a full fuel assembly and an empty fuel assembly.

Although the data were not discussed in this paper, we have also compared thermal neutron interrogation data for the separation of interrogating neutrons from fission neutrons. Again, the synchronous detection method is better than conventional background separation (that is, actively assay a sample, then interrogate an empty chamber and subtract the two signals). The synchronous detection method in this instance uses the phase difference between the interrogating and fission neutron signals to perform the separation. The synchronous detection method worked better than the conventional separation, but not nearly as well as the separation achieved using methods such as the shuffler (source removal) or the second generation differential die-away machine (using shielded, short die-away detectors).

Although the SAND system cannot replace these machines, it might be used in conjunction with assay systems that presently use conventional subtraction to remove the interrogating and background components. An area for future effort will be exploring other applications in which synchronous detection could be used to enhance existing active neutron methods.

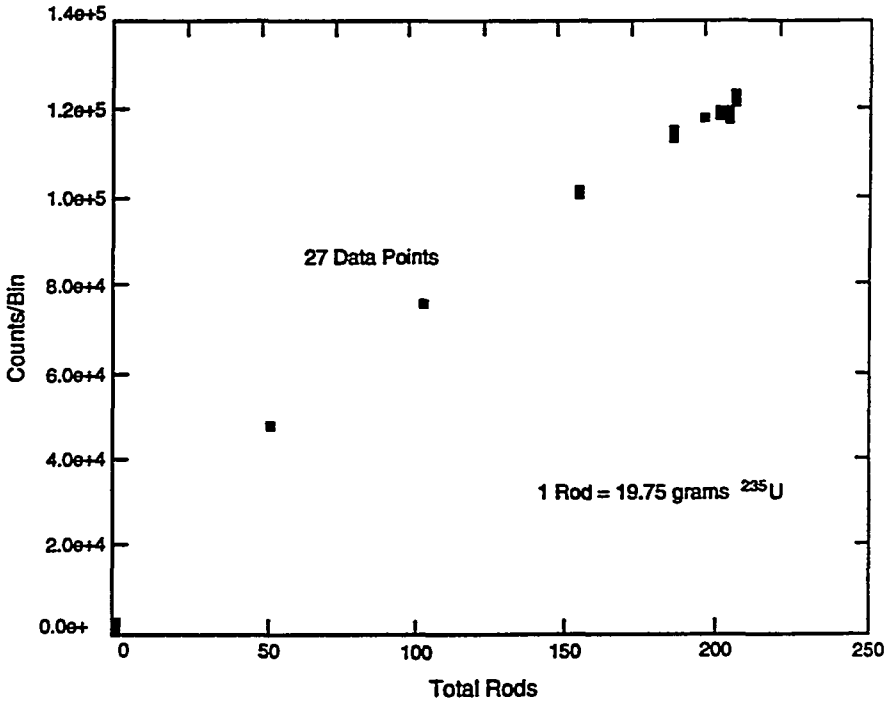

Fig. 14. Results of the SAND assay of fuel rods. The response of the SAND system is plotted as a function of the number of fuel rods.

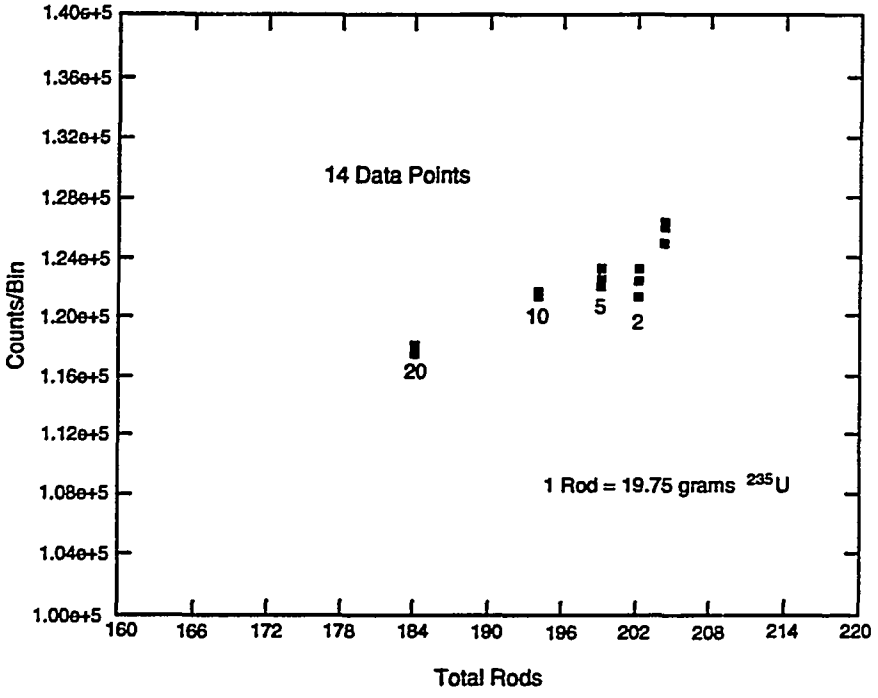

Fig. 15. An expanded view of the assay of fuel rods with the SAND system showing the system response for only the cases close to a full fuel assembly. The number below each cluster of points is the number of rods removed from a full assembly. Different spatial positions were selected for these data.

4. Synchronous detection does not saturate the neutron detectors because the interrogating neutron pulse is a square wave. By contrast, active neutron techniques that interrogate with a short pulse of neutrons often saturate the detectors. Detector saturation introduces a nonlinear effect or forces the counting to begin well after the neutron pulse. In either case, significant information is lost. The synchronous detection method does not suffer this limitation.

5. This particular configuration interrogated the cold fuel with a "hot" neutron spectrum. It is important to interrogate fuel assemblies with nonthermal neutrons so the neutrons penetrate to the core of the assembly. Otherwise, only the outer layer

is measured. Systems that use short-pulse interrogation, such as conventional differential die-away instruments, cannot begin counting until the detectors are no longer saturated. At this point the interrogating spectrum is entirely thermal.

Although the precise neutron energy distribution was not known for these experiments, MCNP calculations shown in Fig. 5 indicate that the interrogating spectrum extends from epi-thermal to the neutron source energy of 14 MeV. Moreover, the measurement seemed insensitive to the position of the individual rods being removed during the cold fuel measurements. However, this area requires additional investigation to quantify the position sensitivity of the assay.

REFERENCES

[1] M. M. Pickrell, M. Mahdavi, and H. Pfutzner, "Investigations of the Performance and Nondestructive Assay Applications of the EMR/Schlumberger Neutron Generator," *Nucl. Mater. Manage.* **XXII** (Proc. Issue), 444-449 (1993).

[2] Steven A. Tretter, *Introduction to Discrete-Tme Signal Processing* (John Wiley & Sons, New York, 1976).

[3] Allan V. Oppenheim and Alan S. Willsky, *Signals and Systems* (Prentice-Hall, Inc., Englewood Cliffs, N. J., 1983).

[4] *Stanford Research Systems Catalog: Scientific and Engineering Instruments.* (Stanford Research Systems, Sunnyvale, CA, 1992-1993), pp. 56-70.

[5] T. D. Reilly, N. Ensslin, H. A. Smith, Jr., and S. Kreiner, Eds., *Passive Nondestructive Assay of Nuclear Materials* (Washington, Government Printing Office, 1991) NUREG/CR-5550, Los Alamos National Laboratory document LA-UR-90-732 (1991).

[6] H. O. Menlove, J. K. Halbig, G. E. Bosler, P. M. Rinard, and S. W. O'Rear, Jr., "The Design and Calibration of the Spent-Fuel Neutron Coincidence Counter for Underwater Applications," Los Alamos National Laboratory report LA-12769-MS (May 1994).

[7] N. Miura and H. O. Menlove, "The Use of Curium Neutrons to Verify Plutonium in Spent Fuel and Reprocessing Wastes," Los Alamos National Laboratory report LA-12774-MS (May 1994).

[8] G. Bignan, J. Capsie, J. R. Dherbey, and P. M. Rinard, "A Comparison of Spent Fuel Assembly Control Instruments: The Cadarache Python and the Los Alamos FORK," in *Fourth International Conference on Facility Operations—Safeguards Interface* (American Nuclear Society, La Grange Park, Illinois, 1991), pp. 245-250.

[9] S. T. Hsue, T. W. Crane, W. L. Talbert, Jr., and J. C. Lee, "Nondestructive Assay Methods for Irradiated Nuclear Fuels," Los Alamos Scientific Laboratory report LA-6923 (January 1978).

[10] P. M. Rinard, "Spent-Fuel Verification with the Los Alamos Fork Detector," Los Alamos National Laboratory document LA-UR-87-2970 (September 1987).

[11] D. D. Cobb, J. R. Phillips, G. E. Bosler, G. W. Eccleston, et al., "Nondestructive Verification and Assay Systems for Spent Fuels," Los Alamos National Laboratory report LA-9041 (April 1982). Volumes 1 and 2.

[12] T. K. Li, J. L. Parker, H. G. Wagner, J. Goerten, et al., "Plutonium Analysis of High-Burnup Spent-Fuel Dissolver Solutions by Low-Energy Gamma-Ray Spectrometry," in *Proc. 15th ESARDA Symposium of Safeguards and Nucl. Mater. Manage.* (Joint Research Centre, Rome, Italy, 1993) ESARDA **26**, pp. 297-501.

[13] H. O. Menlove, J. E. Stewart, S. Z. Qiao, T. R. Wenz, and G. P. D. Verrecchia, "Neutron Collar Calibration and Evaluation for Assay of LWR Fuel Assemblies Containing Burnable Neutron Absorbers," Los Alamos National Laboratory report LA-11965-MS (November 1990).

[14] A. J. Nelson, G. E. Bosler, R. H. Augustson, and L. R. Cowder, "Underwater Measurement of a 15 x 15 MOX PWR-Type Fuel Assembly," Los Alamos National Laboratory report LA-11850-MS (December 1990).

[15] H. O. Menlove, "Description and Performance Characteristics of the Neutron Coincidence Collar for the Verification of Reactor Fuel Assemblies," Los Alamos National Laboratory report LA-8939-MS (August 1981).

[16] T. C. Piper, R. J. Kirkham, G. W. Eccleston, and H. O. Menlove, "Analysis of Spent, Highly Enriched Reactor Fuel by Delayed Neutron Interrogation," in *Proc. of the American Nuclear Society International Topical Meeting on Safety Margins in Criticality Safety* (American Nuclear Society, San Francisco, 1989) p. 168.

[17] T. C. Piper and R. J. Kirkham, "Systems Report on the Analysis of Spent, Highly Enriched U-235 Reactor Fuel by Delayed Neutron Interrogation," Idaho National Engineering Laboratory technical report WINCO-1076 (May 1990).

[18] P. M. Rinard, E. L. Adams, H. O. Menlove, and J. K. Sprinkle, Jr, "Nondestructive Assays of 55-Gallon Drums Containing Uranium and Transuranic Waste Using Passive/Active Shufflers," *Nucl. Mater. Manage.* **XXI** (Proc. Issue), 187-195 (1992).

[19] P. M. Rinard, "Shuffler Instruments for the Nondestructive Assay of Fissile Materials," Los

Alamos National Laboratory report LA-12105 (May 1991).

[20] M. S. Krick, L. R. Cowder, V. Maltsev, A. Chernikev, et al., "Active Well Coincidence Counter Measurements of Enriched Uranium Fuel Assemblies in Scanning and Stationary Modes," Los Alamos National Laboratory report LA-12224-MS (December 1991).

[21] N. Ensslin, M. S. Krick, D. G. Langer, D. W. Miller, and M. C. Miller, "Measurement of the Assay Precision of the Active Neutron Multiplicity Technique," *Nucl. Mater. Manage.* **XXI** (Proc. Issue) 785-789 (1992).

[22] J. T. Caldwell, J. M. Bieri, T. H. Kuckertz, M. R. Newell, et al., "Greatly Improved Transuranic Waste Assay Accuracy Using Neutron Signal Imaging," *Fouth International Conference on Facility Operations—Safeguards Interface* (American Nuclear Society, La Grange Park, Illinois, 1991).

[23] P. M. Rinard, E. L. Adams, H. O. Menlove, and J. K. Sprinkle, Jr. "Characterizing and Improving Passive-Active Shufflers for Assays of 208-Liter Waste Drums," *Proc. 14th ESARDA Symposium of Safeguards and Nucl. Mater. Manage.* (Saimanca, Spain, May 1992); Los Alamos National Laboratory document LA-UR-92-1252.

[24] J. T. Caldwell, R. D. Hastings, G. C. Herrera, W. E. Kunz, and E. R. Shunk, "The Los Alamos Second-Generation System for Passive and Active Neutron Assays of Drum-Size Containers," Los Alamos National Laboratory report LA-10774-MS (September 1986).

[25] P. M. Rinard, E. L. Adams, H. O. Menlove, and J. K. Sprinkle, Jr. "The Nondestructive Assay of 55-Gallon Drums Containing Uranium and Transuranic Waste Using Passive-Active Shufflers," Los Alamos National Laboratory report LA-12446-MS (November 1992).

[26] K. L. Coop. "A Combined Thermal/Epithermal Neutron Interrogation Device To Assay Fissile Materials In Large Waste Containers," In *Proceedings of the 11th Annual ESARDA Symposium on Safeguards and Nuclear Material Management* (Luxembourg, Commission of the European Communities, 1989). pp. 201-206,

[27] Harl 'O M. Fisher, "A Nuclear Cross Section Data Handbook," Los Alamos National Laboratory report LA-11711-M (December 1989).

[28] *ACE-MCS Operator's Manual.* EG&G Ortec Part No. 736790, EG&G Ortec, Inc., 1990.

[29] Judith F. Briesmeister, Ed., "MCNP - A General Monte Carlo Code for Neutron and Photon Transport, Version 3A," Los Alamos National Laboratory report LA-7396-M, Rev. 2 (September 1986).